Screened Lamb Shift Calculations for Lithiumlike Uranium, Sodiumlike Platinum, and Copperlike Gold

K. T. Cheng
University of California, Lawrence Livermore National Laboratory, P.O. Box 808, Livermore, California 94550

W. R. Johnson and J. Sapirstein
Department of Physics, University of Notre Dame, Notre Dame, Indiana 46556
(Received 25 March 1991)

Calculations of the screened electron self-energy are carried out in local central potentials that approximate a Hartree-Fock potential. The resulting energy corrections are combined with screened vacuum-polarization calculations and used to predict the Lamb shift for $n=2$ states of lithiumlike uranium, $n=3$ states of sodiumlike platinum, and $n=4$ states of copperlike gold. The theoretical values of the screened Lamb shift are found to be in good agreement with values inferred from experiments.

PACS numbers: 31.30.Jv, 12.20.Ds, 31.20.Tz

An outstanding problem in atomic physics is the correct treatment of relativistic and quantum electrodynamic (QED) effects in many-electron atoms. In neutral atoms, with the exception of hydrogen and helium, the large numerical uncertainties accompanying the solution of the Schrödinger equation obscure these normally small effects. However, the study of the spectroscopy of highly charged ions allows the investigation of this fundamental problem in a particularly clear fashion. This is, first, because of the great enhancement of these effects as the nuclear charge grows: The hydrogenic Lamb shift, for example, scales as Z^4. Second, the convergence of a particular technique of solving the Schrödinger equation, relativistic many-body perturbation theory (MBPT), becomes very rapid because each higher order of MBPT is accompanied by an additional factor $1/Z$. It has recently been shown that for highly charged ions of the lithium,[1] sodium,[2] and copper[3] isoelectronic sequences, QED corrections to valence electron energies can be unambiguously isolated by comparing experimental transition energies with the results of MBPT, which include the effects of the Coulomb and Breit interactions but omit the QED corrections. These corrections are dominated by the Feynman graphs of Fig. 1, which describe the point-Coulomb Lamb shift when the electron moves in the Coulomb field of a point nucleus of charge Z. However, this shift is larger than the actual QED correction, which we refer to as the screened Lamb shift. Although the resulting experimental values of the screened Lamb shift can be accounted for phenomenologically[4-6] using various modifications of the point-Coulomb Lamb-shift data,[7,8] it is necessary to calculate the QED corrections from first principles to obtain an understanding of the Lamb shift at a fundamental level.

Our point of departure is a perturbation expansion of the QED S matrix in the Furry[9] representation, with the nuclear Coulomb potential replaced by a suitable atomic potential $V(r)$. This expansion contains the Coulomb and Breit interaction terms of the relativistic MBPT expansion, together with other terms of field-theoretic origin, not included in MBPT.[10] The lowest-order terms not included in MBPT are the electron self-energy and vacuum-polarization corrections shown in Figs. 1(a) and 1(b), with the electron propagator now describing an electron moving in a non-Coulomb potential $V(r)$. We refer to these corrections as the screened self-energy and screened vacuum polarization, respectively. While we will show in this Letter that these graphs account for the bulk of the screened Lamb shift, we note that there are also contributions from higher-order graphs, which will be discussed at the end of the Letter.

Our calculations of the self-energy in a non-Coulomb potential are based on a method introduced by Brown, Langer, and Schaefer[11] to treat the electron self-energy numerically, and used by others[12-15] to study self-energy corrections for $1s$ electrons in the strong Coulomb fields of high-Z nuclei. This method is generalized here to treat electronic states with principal quantum numbers $n>1$.

While MBPT calculations for the ions considered here were carried out starting with a V^{N-1} Hartree-Fock (HF) potential, the QED calculations assume a local potential. In the present work we use local potentials that give eigenenergies close to HF values. Specifically, we use both an HF potential with Kohn-Sham average ex-

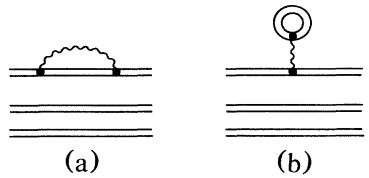

FIG. 1. Self energy and vacuum-polarization graphs. The double line indicates propagation of the electron in an external potential $V(r)$.

change interaction, and a Hartree-like potential defined by

$$V(r)=V_{\rm nuc}(r)+\sum_a (2j_a+1)v_0(a,a:r)\,, \tag{1}$$

where

$$v_0(a,a:r)\equiv\int dr'\frac{1}{r_>}[g_a^2(r')+f_a^2(r')]\,. \tag{2}$$

The core states a are determined self-consistently. Note that we include the effect of finite nuclear size on $V_{\rm nuc}(r)$ by modeling the nucleus as a uniformly charged sphere, using the nuclear radii given in Ref. 8. We found that both potentials gave the same value for the screened Lamb shift to within numerical errors.

An important point of principle is whether QED calculations in non-HF potentials can be consistently joined with the MBPT results calculated starting from the HF potential. To address this point, we note that MBPT expansions for highly charged ions based on local potentials close to a HF potential converge rapidly to the same limit as those based on a HF potential. We have explicitly checked this by carrying out a MBPT calculation through second order for the local potentials used in this work. As expected, the first-order energy correction brings the local potential energies into very close agreement with the HF energies, and the second-order calculation leads to almost exact agreement between the two MBPT calculations.

The formulas for the self-energy calculation are written out in the literature[11,13] and will not be repeated here, but we will remark on some numerical issues. The calculation involves a rotation of the contour of the fourth component of the photon momentum k_0 from the real to the imaginary axis, $k_0\rightarrow i\omega$. An integral over ω from zero to infinity must be evaluated. The integrand involves two radial integrals over wave functions and electron Green's functions, which are represented as an infinite partial-wave expansion. In practice this expansion and the ω integral can be carried out only to a finite number of partial waves and a given energy, respectively, and extrapolation methods must be used to complete the calculation. The errors involved in these methods were sufficiently severe in earlier work to limit the application of the technique to $n=1$ states.

In order to extend this method to states of higher principal quantum number, we first made use of a very fine radial grid. We found that a 4000-point grid allowed the stable generation of the partial-wave expansion of the electron Green's function up to $l=120$, as opposed to the limit of about 20 in earlier work. While this enabled greater accuracy in extrapolating the partial-wave expansion to infinity, its slow falloff as $1/l^2$ still led to significant numerical uncertainties. Therefore, we calculated for the Coulomb case the asymptotic behavior of the ω integrand for large l, which had the remarkably simple, ω-independent form $-(mZ\alpha/\pi)/l^2$. Extrapolating with forms that tended to this limit led to a great increase in accuracy. For the non-Coulomb case, we did not obtain an analytic formula, but used the fact that the $1/l^2$ coefficient was again ω independent, and that at low energies this coefficient could be obtained from a numerical fit with high accuracy. The maximum energy that could be calculated with good accuracy for the ions considered in this work was about $5mc^2$ for $n=2$ states, $3mc^2$ for $n=3$ states, and $2mc^2$ for $n=4$ states. Past those limits 120 partial waves were still nonasymptotic, and control over the partial-wave expansion began to degrade.

The next issue we treated was the accurate evaluation of the ω integration. The integral up to the limits given above could be evaluated with very high accuracy. This was done by dividing the range of integration into several regions, and evaluating the integral in each with more and more Gaussian points until convergence was achieved. The integration from those limits up to infinity, which we refer to as the tail, was by far the dominant source of numerical error, as in previous work. This is because the numerical control of the partial-wave expansion is poorest at the highest-energy points that are used to form a fit to the large-ω behavior, which is then extrapolated to infinity to carry out the tail integration. The procedure we used was to fit with various functions of ω (the leading behavior is $1/\omega^3$), using values of the integrand at the highest possible ω. Errors were estimated from the spread in values of the tail arising from use of different functions. A useful cross-check was ensuring we reproduced within errors the known results for the point-Coulomb case, which have recently been calculated for the $n=3$ and $n=4$ levels.[16,17] The results for the screened self-energy calculation are presented in Table I.

Turning now to the calculation of vacuum polarization in a non-Coulomb potential, we note that this effect is dominated by the Uehling potential. Therefore, we incorporate screening in this potential only, leaving the screening corrections to the higher-order terms of the Wichmann-Kroll[18] expression, which are already quite small, for a later work. The Uehling potential for a distributed charge density $\rho(\mathbf{r})$ is

$$U(r)=-\frac{2\alpha e^2}{3\pi}\int d^3x\frac{\rho(\mathbf{x})}{|\mathbf{r}-\mathbf{x}|}\int_0^\infty dt(t^2-1)^{1/2}\left(\frac{1}{t^2}+\frac{1}{2t^4}\right)e^{-2(mc/\hbar)t|\mathbf{r}-\mathbf{x}|}\,. \tag{3}$$

The density $\rho(\mathbf{r})$ has contributions from the nuclear charge distribution and from the core electrons. We carry out the angular integrations analytically, the t integration using adaptive Gaussian quadrature, and we evaluate the remaining radial integral with standard numerical techniques. The vacuum-polarization contributions determined numerically

TABLE I. Screened Lamb shift contributions. Self-energy and vacuum polarization are from the present calculation: L_{res} sums the Wichmann-Kroll, higher-order, and relativistic-recoil contributions from Ref. 8. Units are a.u.

Ion	State	Self-energy	Vacuum polarization	L_{res}	L_{th}
U^{89+}	$2s_{1/2}$	2.303(2)	−0.579	0.031(5)	1.755(5)
U^{89+}	$2p_{1/2}$	0.316(2)	−0.096	0.007(1)	0.227(2)
Pt^{67+}	$3s_{1/2}$	0.290(3)	−0.056	0.003	0.237(3)
Pt^{67+}	$3p_{3/2}$	0.039(2)	0.000	0.000	0.039(2)
Au^{50+}	$4s_{1/2}$	0.088(1)	−0.017	0.001	0.072(1)
Au^{50+}	$4p_{3/2}$	0.013(1)	0.000	0.000	0.013(1)

from the Uehling potential are listed in Table I.

We are now in a position to compare theory with experiment. A compilation of the various QED contributions to $n=1$ and $n=2$ states has been given in Table II of Ref. 8, which lists various contributions to the Lamb shift for hydrogenlike atoms. The first two are the Coulomb self-energy and its finite-size corrections: The sum of these two is to be replaced by our self-energy calculation, which accounts both for screening and for finite nuclear size. The next two contributions are the Coulomb Uehling potential and its finite-size corrections: Again, these are to be replaced with our screened Uehling calculation. The remaining four contributions are Wichmann-Kroll corrections, an estimate of higher-order terms, finite size of the nucleus, and relativistic recoil. The finite-nuclear-size contribution is already included in MBPT; the other three are summed and listed as residual effects, L_{res}, in Table I. For $n=3$ and $n=4$ states, we assume $1/n^3$ scaling to determine these effects. The sum of our screened self-energy, screened vacuum polarization, and residual effects is our basic result, and is given as L_{th} in Table I.

For lithiumlike uranium (U^{89+}), the measured $2p_{1/2}$-$2s_{1/2}$ transition energy[19] is 280.59 ± 0.10 eV. When the non-QED value of 322.24 eV [which includes 322.37 eV from MBPT (Ref. 20) and −0.13 eV from nuclear polarization[21]] is subtracted from this measurement, an experimental value $L_{expt} = -41.65 \pm 0.10$ eV is found. The energy of the $3p_{3/2}$-$3s_{1/2}$ transition in sodiumlike platinum (Pt^{67+}) has been measured to be 653.44 ± 0.07 eV,[22] and the corresponding value from MBPT is 658.76 eV,[2] leading to an experimental value of the Lamb shift $L_{expt} = -5.32 \pm 0.07$ eV. For copperlike gold (Au^{50+}) the experimental $4p_{3/2}$-$4s_{1/2}$ transition energy is 253.40 ± 0.08 eV,[23] and the theoretical energy is 254.98 ± 0.01 eV,[3] leading to an experimental Lamb shift $L_{expt} = -1.58 \pm 0.09$ eV. We compare these numbers to our theoretical values in Table II.

There has been a calculation on lithiumlike uranium by Indelicato and Mohr[24] that is closely related to the present one. To compare with this calculation we redid our self-energy calculation assuming a point nucleus with and without screening. The difference corresponds to the terms $2E_{2s}^{(1s)}$ and $2E_{2p}^{(1s)}$ in Ref. 24. We find reasonable agreement, −2.82(5) eV and −0.94(19) eV, compared to −2.88 eV and −0.64 eV from Ref. 24. We note that when we compared our two screened calculations with and without nuclear size, we found a distinctly smaller nuclear-size effect than that given in Ref. 8; specifically, 0.6 eV versus 1.0 eV.

The agreement with experiment found here is quite good, particularly for uranium. However, a set of higher-order Feynman graphs must be considered before one can claim a fundamental understanding of these transitions. As mentioned above, Furry-representation QED provides a rigorous theoretical framework for calculating the spectrum of highly charged ions, justifying the use of MBPT and providing an unambiguous set of Feynman graphs associated with the Lamb shift. We have evaluated the most important such graphs, the self-energy and the vacuum polarization. Two examples of graphs that we have omitted are shown in Fig. 2. The evaluation of these graphs involve the same sort of technology used here, but a complete evaluation of them has not been made at the present time. However, a part of Fig. 2(a) corresponding to the screening of the $1s$ self-energy by the outer $2s$ and $2p$ electrons has been evaluated in Ref. 24 for lithiumlike uranium, where a 0.3-eV contribution to the $2s$-$2p$ shift was found. Because we already have agreement between theory and experiment

TABLE II. Comparison of experiment with theory. Units are eV.

Ion	Transition	Expt.	MBPT	L_{expt}	L_{th}
U^{89+}	$2p_{1/2}$-$2s_{1/2}$	280.59(10)	322.24	−41.65(10)	−41.57(15)
Pt^{67+}	$3p_{3/2}$-$3s_{1/2}$	653.44(7)	658.76	−5.32(7)	−5.41(12)
Au^{50+}	$4p_{3/2}$-$4s_{1/2}$	253.40(8)	254.98(1)	−1.58(9)	−1.61(4)

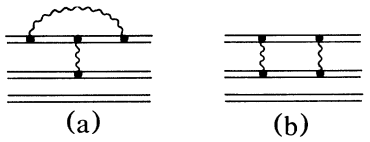

FIG. 2. Sample higher-order graphs contributing to the screened Lamb shift.

at below this level, this is an indication that significant cancellations are to be expected in the complete calculation. The next stage of research in this problem must focus on verifying this conclusion. Until those large-scale calculations are carried out, we simply observe that evaluating the Lamb shift in realistic potentials, coupled with high-accuracy MBPT calculations, gives very good agreement with experiment. If it can be shown that the remaining graphs are indeed small, the relativistic many-body problem will have been shown to be understood at the tenth of an eV level in highly charged ions.

We would like to thank Steven Blundell, Peter Mohr, Neal Synderman, and Donald Yennie for valuable discussions. A particular debt of thanks is due to G. E. Brown, who provided valuable encouragement. The work of W.R.J. and J.S. was supported in part by NSF Grant No. PHY-90-12408, and that of K.T.C. by the DOF under Contract No. W-7405-ENG-48. W.R.J. and J.S. acknowledge the hospitality of LLNL during the course of this work. Some of the calculations were carried out on the National Center for Supercomputer Applications CRAY Y-MP computer.

[1]W. R. Johnson, S. A. Blundell, and J. Sapirstein, Phys. Rev. A **37**, 2664 (1988).

[2]W. R. Johnson, S. A. Blundell, and J. Sapirstein, Phys. Rev. A **38**, 2699 (1988).

[3]W. R. Johnson, S. A. Blundell, and J. Sapirstein, Phys. Rev. A **42**, 1087 (1990).

[4]J. F. Seely, Phys. Rev. A **39**, 3682 (1989).

[5]J. F. Seely and R. A. Wagner, Phys. Rev. A **41**, 5246 (1990).

[6]Y. K. Kim, D. H. Baik, P. Indelicato, and J. P. Desclaux, Phys. Rev. A (to be published).

[7]P. J. Mohr, At. Data Nucl. Data Tables **29**, 453 (1983).

[8]W. R. Johnson and G. Soff, At. Data Nucl. Data Tables **33**, 405 (1985).

[9]W. H. Furry, Phys. Rev. **81**, 115 (1951).

[10]J. Sapirstein, Nucl. Instrum. Methods B **43**, 338 (1989).

[11]G. E. Brown, J. S. Langer, and G. W. Schaefer, Proc. Roy. Soc. London A **251**, 92 (1959).

[12]G. E. Brown and D. F. Mayers, Proc. Roy. Soc. London A **251**, 105 (1959).

[13]A. M. Desiderio and W. R. Johnson, Phys. Rev. A **3**, 1267 (1971).

[14]K. T. Cheng and W. R. Johnson, Phys. Rev. A **14**, 1943 (1976).

[15]G. Soff, P. Schlüter, B. Müller, and W. Greiner, Phys. Rev. Lett. **48**, 1465 (1982).

[16]P. J. Mohr and Y.-K. Kim (private communication).

[17]S. A. Blundell and N. Synderman, LLNL report, 1991 (to be published).

[18]E. Wichmann and N. Kroll, Phys. Rev. **101**, 843 (1956).

[19]J. Schweppe, A. Belkacem, L. Blumenfeld, Nelson Claytor, B. Feinberg, Harvey Gould, V. E. Kostroun, L. Levy, S. Mishawa, J. R. Mowat, and M. Prior, Phys. Rev. Lett. **66**, 1434 (1991).

[20]S. A. Blundell, W. R. Johnson, and J. Sapirstein, Phys. Rev. A **41**, 1698 (1990).

[21]G. Plunien, B. Müller, W. Greiner, and G. Soff, Phys. Rev. A **39**, 5428 (1989).

[22]T. E. Cowan, C. L. Bennett, D. D. Dietrich, J. Bixler, C. J. Hailey, J. R. Henderson, D. A. Knapp, M. A. Levine, R. E. Marrs, and M. B. Schneider, Phys. Rev. Lett. **66**, 1150 (1991).

[23]J. F. Seely, C. M. Brown, and U. Feldman, At. Data Nucl. Data Tables **43**, 145 (1989).

[24]P. Indelicato and P. J. Mohr, Theor. Chim. Acta. (to be published).